

Chloroplast division site placement requires dimerization of the ARC11/AtMinD1 protein in *Arabidopsis*

Makoto T. Fujiwara^{1,2,‡}, Ayako Nakamura², Ryuichi Itoh^{2,*}, Yukihiisa Shimada², Shigeo Yoshida² and Simon Geir Møller^{1,‡}

¹Department of Biology, University of Leicester, University Road, Leicester, LE1 7RH, UK

²Plant Functions Laboratory and Plant Science Center, RIKEN, Hirosawa 2-1, Wako, Saitama 351-0198, Japan

*Present address: Department of Chemistry, Biology and Marine Science, University of the Ryukyus, Nishihara, Okinawa 903-0213, Japan

‡Authors for correspondence (e-mail: mtf1@mac.com; sgm5@le.ac.uk)

Accepted 9 January 2004

Journal of Cell Science 117, 2399-2410 Published by The Company of Biologists 2004
doi:10.1242/jcs.01092

Summary

Chloroplast division is mediated by the coordinated action of a prokaryote-derived division system(s) and a host eukaryote-derived membrane fission system(s). The evolutionary conserved prokaryote-derived system comprises several nucleus-encoded proteins, two of which are thought to control division site placement at the midpoint of the organelle: a stromal ATPase MinD and a topological specificity factor MinE. Here, we show that *arc11*, one of 12 recessive *accumulation and replication of chloroplasts (arc)* mutants in *Arabidopsis*, contains highly elongated and multiple-arrayed chloroplasts in developing green tissues. Genomic sequence analysis revealed that *arc11* contains a missense mutation in α -helix 11 of the chloroplast-targeted AtMinD1 changing an Ala at position 296 to Gly (A296G). Introduction of wild-type AtMinD1 restores the chloroplast division defects of *arc11* and quantitative RT-PCR analysis showed that the degree of complementation was highly dependent on transgene expression levels. Overexpression of the mutant *ARC11/AtMinD1* in transgenic plants results in the

inhibition of chloroplast division, showing that the mutant protein has retained its division inhibition activity. However, in contrast to the defined and punctate intraplasmidic localization patterns of an AtMinD1-YFP fusion protein, the single A296G point mutation in ARC11/AtMinD1 results in aberrant localization patterns inside chloroplasts. We further show that AtMinD1 is capable of forming homodimers and that this dimerization capacity is abolished by the A296G mutation in ARC11/AtMinD1. Our data show that *arc11* is a loss-of-function mutant of *AtMinD1* and suggest that the formation of functional AtMinD1 homodimers is paramount for appropriate AtMinD1 localization, ultimately ensuring correct division machinery placement and chloroplast division in plants.

Supplemental data available online

Key words: *Arabidopsis*, Chloroplast division, Min system, *arc* mutant

Introduction

Chloroplasts, photosynthetic organelles in plants, have evolved from an ancestral cyanobacterium harboring their own genomes and internal membrane systems related to the components of modern cyanobacteria (Gray, 1999). During evolution, the majority of prokaryotic genes were lost or transferred from chloroplasts to the eukaryotic host nuclei, adapting to eukaryotic gene expression systems and gaining cellular functions by targeting their gene products to chloroplasts or other subcellular compartments (Martin et al., 2002). However, not only cyanobacterial-derived but also a number of non-cyanobacterial-like proteins are thought to be targeted to chloroplasts (Martin et al., 2002), implying that modern chloroplasts are maintained by processes that require inherent prokaryotic and acquired eukaryotic systems.

Chloroplast division is an integral part of chloroplast development (Pyke, 1999), and chloroplasts divide from pre-existing plastids by binary fission (Leech and Pyke, 1988; Kuroiwa et al., 1998; Pyke, 1999; Hashimoto, 2003). It has

recently been shown that chloroplast division represents a multifaceted process involving complex interdependency of both bacterial/cyanobacterial-derived and eukaryotic proteins (Hashimoto, 2003; Miyagishima et al., 2003; Gao et al., 2003).

Because of the involvement of bacterial/cyanobacterial-like proteins during chloroplast division, bacterial cell division has been used as a paradigm in dissecting the mechanism of chloroplast division. The bacterial-like *FtsZ* gene, *AtFtsZ1-1*, was the first nuclear-encoded chloroplast division component identified from *Arabidopsis thaliana* (Osteryoung and Vierling, 1995; Osteryoung et al., 1998), and most plants contain nuclear genes with high similarity to the bacterial cell division proteins FtsZ, MinD and MinE (Strepp et al., 1998; Osteryoung et al., 1998; Beech et al., 2000; Colletti et al., 2000; Itoh et al., 2000; Maple et al., 2002). Bacterial cell division is initiated by FtsZ, a cytoplasmic tubulin-like GTPase that assembles into a cytokinetic ring (Z-ring) at midcell in order to recruit other cell division proteins (Bi and Lutkenhaus, 1991; Erickson et al., 1996; Rothfield et al., 1999). Spatial regulation of Z-ring

formation depends on the *minB* operon-encoded proteins, MinC, MinD and MinE, mutations of which result in asymmetrical cell division, formation of anucleate minicells and filamentation (de Boer et al., 1989). MinD is a membrane-associated ATPase and functions as an inhibitory cell division regulator by forming a complex with the division inhibitor MinC in the presence of ATP, thereby preventing FtsZ polymerization (de Boer et al., 1991; Huang and Lutkenhaus, 1996; Hu et al., 1999). MinCD activity is dynamically controlled by the topological specificity factor MinE. MinE stimulates MinD ATPase activity and subsequent membrane release, allowing MinCD oscillatory behavior, which ensures division initiation only at midcell (Raskin and de Boer, 1997; Raskin and de Boer, 1999; Hu and Lutkenhaus, 2001; Fu et al., 2001; Hale et al., 2001; Margolin, 2001; Lutkenhaus and Sundaramoorthy, 2003). It has recently been reported that MinD assembles into a dimer or polymer in the presence of ATP (Hu et al., 2002; Suefuji et al., 2003; Hu and Lutkenhaus, 2003), which is predicted to be important for its function (Lutkenhaus and Sundaramoorthy, 2003).

AtMinD1, a *MinD* homolog, was isolated from *Arabidopsis* and its role in chloroplast division was established by observations revealing that transgenic plants with reduced *AtMinD1* levels show asymmetric chloroplast division, whereas elevated *AtMinD1* levels show chloroplast division inhibition (Colletti et al., 2000; Kanamaru et al., 2000; Dinkins et al., 2001). More recently, the *minE* homolog *AtMinE1* was identified in *Arabidopsis* (Itoh et al., 2001; Maple et al., 2002) and its role in chloroplast division site determination has been shown where *AtMinE1* overexpression results in loss of topological specificity (Maple et al., 2002). Taken together, these studies, in addition to studies on plant FtsZ proteins, show that the prokaryotic part of the chloroplast division machinery is essential during the initiation stage of chloroplast division (Vitha et al., 2001; Kuroiwa et al., 2002; Miyagishima et al., 2003). In addition to Min protein homologs the bacterial/cyanobacterial origin of the division process has been further underlined by the identification of *ARTEMIS* (Fulgosi et al., 2002) and the *Synechococcus* Ftn2-like protein (Vitha et al., 2003). However, to date the underlying molecular mechanisms of chloroplast division remain unknown.

Twelve recessive *accumulation and replication of chloroplasts (arc)* mutants, showing altered number and morphology of chloroplasts in mesophyll cells, have been identified from *Arabidopsis* (Pyke, 1997; Pyke, 1999; Marrison et al., 1999). Among them, *arc11* is unique in that it produces a reduced and heterogeneous population of chloroplasts in mesophyll cells (Marrison et al., 1999). *arc11* was originally isolated from *Ler* transposon insertion lines and was mapped to *Arabidopsis* chromosome V, but was shown not to be associated with the transposon (Marrison et al., 1999).

In this study we begin to unravel the underlying molecular mechanism of chloroplast division site placement in *Arabidopsis*. We show that the *arc11* mutant phenotype is derived from a single point mutation in the *AtMinD1* gene and that *arc11* chloroplasts show remarkable defects in division site placement, an observation previously not reported. We further reveal that *AtMinD1* can form homodimers but that dimerization is abolished by the single point mutation found in *AtMinD1*. Moreover, the mutated ARC11 protein shows aberrant intraplasmic localization patterns, suggesting that

AtMinD1 dimerization and appropriate localization is vital for correct chloroplast division in *Arabidopsis*.

Materials and Methods

Plant materials and growth conditions

Seeds of *A. thaliana* ecotypes Landsberg *erecta* (*Ler*) and Columbia (*Col*) and the *arc11* mutant (Marrison et al., 1999) (*Ler* background, Ohio State University, USA) were surface-sterilized with 70% (v/v) ethanol and 1% (w/v) sodium hypochlorite, 0.2% (v/v) Tween-20, and sown on 0.8% (w/v) agar-containing Murashige-Skoog (MS) medium (Wako Jun-yaku, Japan) supplemented with Gamborg's B5 vitamins (Wako Jun-yaku) and 1% (w/v) sucrose. Seeds of *Nicotiana tabacum* cultivar bright yellow 4 were also surface-sterilized and sown on MS agar medium supplemented with B5 vitamins and 3% (w/v) sucrose. Plants were grown in plant growth incubators at 22°C for *Arabidopsis* and 28°C for tobacco under continuous white light illumination (100 $\mu\text{E}/\text{m}^2\text{second}$).

Microscopy

Whole plant seedlings or organs were mounted under glass coverslips, and observed using confocal laser scanning microscopy (CLSM) (TCS-NT, Leica Microsystems, Germany) (Fujiwara and Yoshida, 2001) or epifluorescence microscopy (TE2000, Nikon, Japan, equipped with a Hamamatsu ORCA-ER; IX70, Olympus, Japan, equipped with an Olympus DP50-C). Digital images were imported into the RGB channels of Adobe Photoshop ver. 6.0 (Adobe Systems, USA).

Genomic DNA sequencing of *AtMinD1*

Total DNA from *Col*, *Ler* and *arc11* was extracted using the DNeasy Plant Mini Kit (Qiagen, Germany). The genomic copy of *AtMinD1* was PCR amplified using *PfuTurbo* DNA polymerase (Stratagene, USA) and the oligonucleotide primers, MDF 5'-ACGCTCAG-AAACATTTCTGTC-3' and MDR 5'-CGTTCGGTTCGGTTCG-ATC-3'. The PCR product (1.1 kb) was subjected to direct DNA sequencing. The Monsanto *Arabidopsis* Landsberg Sequence (<http://www.arabidopsis.org/>) was utilized to compare *AtMinD1* sequences between ecotypes.

Complementation analysis

Wild-type *AtMinD1* was expressed, fused to the N-terminus of a double influenza hemagglutinin (dHA)-epitope tag, under the control of the *AtMinD1* upstream genomic promoter region. Two complementary oligonucleotide primers, for a dHA epitope (YPYDVPDYAGYPYDVPDYAG), were annealed and introduced into the *Bam*HI site of pBluescript II SK+ (Stratagene, USA) to yield pSK-HA. A 1.9 kb *Col* genomic DNA fragment, amplified by PCR with MD-HindIII 5'-GGAAGCTTTGGATATCTTGATC-3' (restriction site underlined) and MD3 5'-ATGGATCCGCCAAA-GAAAGAGAAGAAGC-3', was digested with *Bam*HI and *Hind*III and ligated into pSK-HA to yield pMD-HA. A 1.9 kb *Hind*III-*Sac*I fragment of pMD-HA, comprising a 0.9 kb upstream genomic region of *AtMinD1*, the *AtMinD1* ORF and a dHA-coding sequence, was introduced into the pBI-Hyg/35S-NosT vector (Yamaguchi et al., 1999) by simultaneously removing the CaMV35S promoter to yield pBIH-MD-HA. pBIH-MD-HA was employed for *Agrobacterium*-mediated *Arabidopsis* transformation by the floral dip method (Clough and Bent, 1998; Itoh et al., 2001). A total of 55 transformed (T_1) seedlings were selected on MS plates containing hygromycin (25 $\mu\text{g}/\text{l}$, Boehringer Mannheim, Germany), and T_2 to T_4 progenies were used for microscopic characterizations. Stable T_4 seedlings, grown on antibiotic-free MS plates were subjected to quantitative RT-PCR analysis.

Real-time quantitative RT-PCR

Real-time RT-PCR was employed to quantify transcript levels of *AtMinD1* in *Ler*, *arc11* and transgenic plants (Shimada et al., 2003). Total RNA was extracted from 15-day-old seedlings using the guanidine-hydrochloride method, and complementary DNAs (cDNAs) were synthesized from DNase I-treated RNA with random primers using the Super Script First-strand Synthesis System (Invitrogen Life Technologies, USA) (Shimada et al., 2003). Quantitative RT-PCR was performed with a model 7700 sequence detector and a TaqMan Universal PCR Master Mix (Applied Biosystems, USA). Total *AtMinD1* transcripts were monitored using *AtMinD1*-specific PCR primers, MD-FOR 5'-AGAGAGACCGACATTTGCG-3' and MD-REV 5'-CGCGTATCGTCGTTATCACCT-3', and a TaqMan probe MD-TAQ 5'-FAM (6-carboxyfluorescein)-TCGTCCTTCCAACA-CCGCCTTTTCCTAMRA-3' (6-carboxytetramethylrhodamine), and endogenous *AtMinD1* transcripts were monitored using *AtMinD1* mRNA 3'-untranslated region (UTR)-specific primers MD-FOR2 5'-TCCTAGGACAATGTGGAATTCTACTG-3' and MD-REV2 5'-CAGAAATCAAGAACCTCAAGAACAAA-3', and a TaqMan probe MD-TAQ2 5'-FAMTGTGGCTGAGTTCAAGCTCTGATTCT-TATGCCTAMRA-3'. The 18S ribosomal RNA was employed as an internal control.

Overexpression of *AtMinD1*(A296G)

The entire coding sequence of *AtMinD1* was amplified by PCR from *arc11* genomic DNA with MD-*XbaI* 5'-ATTCTAGATCTGTGGAGACAGCTGAAG-3' and MD-*SacI* 5'-TCCGAGCTCCATTAGCCGCCAAAGAA-3'. A 1.0 kb PCR product was digested with *XbaI* and *SacI* and introduced into pBI-Hyg/35S-NosT under the control of the cauliflower mosaic virus 35S (CaMV35S) promoter to yield pBIH-arc11. pBIH-arc11 was employed for *Agrobacterium*-mediated *Arabidopsis* transformation. A total of 20 T₁ seedlings were selected on MS plates containing kanamycin (50 µg/l, Nacalai Tesque, Japan) or hygromycin (25 µg/l, Boehringer). Hypocotyls and primary leaves of T₂ and T₃ seedlings were used for microscopic characterizations. Stable T₃ seedlings were subjected to RT-PCR analysis.

Expression of fluorescent protein fusions

Full-length *AtMinD1* and *AtMinD1*(A296G) proteins were transiently expressed as green fluorescent protein (GFP) or yellow fluorescent protein (YFP) fusions in planta. pGFP2/*AtMinD1* was used as an original vector (Maple et al., 2002). To construct pGFP2/*AtMinD1*(A296G), the entire coding region of *AtMinD1*(A296G) was amplified with MIN/1 and MIN/5 (Maple et al., 2002), digested with *XhoI* and *KpnI*, and ligated into pGFP2 (Kost et al., 1998). Expression vectors for YFP fusion proteins were made from the GFP expression vectors, by replacing the GFP coding sequence with that of YFP (EYFP, Clontech). To verify the N-terminal extensions of *AtMinD1* for a chloroplast targeting transit peptide, the 64 amino acid-coding sequence of *AtMinD1* was amplified by PCR using MD-*SaI* (Kanamaru et al., 2000) and MD-*NcoI* 5'-TTCCCATGGTG-ATAACGACGATACG-3'. The PCR product was digested with *SaI* and *NcoI* and ligated into the CaMV35S-sGFP(S65T)-NOS (Niwa et al., 1999). The expression vectors were introduced into young tobacco leaf cells by particle bombardment. Over 30 cells were analyzed by epifluorescence microscopy using a Nikon TE2000.

Yeast two-hybrid assay

Saccharomyces cerevisiae strain AH109 (MATa, trp1-901, leu2-3, 112, ura3-52, his3-200, gal4Δ, gal80Δ, LYS2::GAL1_{UAS}-GAL1_{TATA}-HIS3, GAL2_{UAS}-GAL2_{TATA}-ADE2, URA3::MEL1_{UAS}-MEL1_{TATA}-lacZ, MEL1) and plasmids pGADT7 and pGBKT7 encoding the Gal4 activation domain and the Gal4 DNA binding domain,

respectively, were derived from MATCHMAKER Two-Hybrid System ver. 3 (Clontech Laboratories, USA). Full-length coding sequences of *AtMinD1* and *AtMinD1*(A296G) were PCR amplified using MIND/5 5'-TACATATGGCGTCTCTGAGATTGTTC-3' and MIND/7 5'-ATGGATCCTTAGCCGCCAAAGAAAGAGAAGAA-GCC-3', digested with *NdeI* and *BamHI*, and ligated into pGADT7 or pGBKT7. Yeast AH109 was cotransformed with pGADT7- and pGBKT7-derived constructs by electroporation. pGADT7-Rec and SV40 Large-T antigen PCR fragment and pGBKT7-53 (Clontech), and pGADT7 and pGBKT7 empty vectors, were also cotransformed as a positive and a negative control, respectively. A pGADT7-derived vector containing an *Arabidopsis* cDNA, which was isolated as a candidate for an *AtMinD1* interacting protein in the two-hybrid screen (M.T.F. and S.G.M., unpublished), was cotransformed with pGBKT7-*AtMinD1* as a weak positive control. Transformants were selected on yeast dropout (SD) media plates lacking leucine (Leu) and tryptophan (Trp) (Clontech), and fresh colonies were then streaked on SD plates lacking Leu, Trp and histidine (His). Cells were cultured on plates for 4 to 9 days at 26-30°C. Yeast growth was classified into four classes based on histidine auxotrophy from three independent experiments: +++, positive growth distinguished 2 days after culture; ++, 3 days; +, 5-6 days; -, normal background growth.

Fluorescence Resonance Energy Transfer (FRET) assay

Expression vectors for *AtMinD1*-CFP (cyan fluorescent protein) and *AtMinD1*-YFP were constructed from pGFP2/*AtMinD1*, by replacing the GFP coding sequence with those of CFP (ECFP, Clontech) and YFP (EYFP, Clontech), respectively. For single and dual expression of *AtMinD1*-CFP and/or *AtMinD1*-YFP, plasmid DNA was introduced into tobacco leaf cells by particle bombardment as described above. FRET assays between fluorophores, CFP (donor) and YFP (acceptor), were performed with a Nikon TE2000, a Hamamatsu ORCA-ER cooled CCD camera and the OpenLab (Improvision, Coventry, UK) system software using 60× N.A. 1.4 objective lens (Nikon) and filters for CFP (exciter S436/10, emitter S470/30) and YFP (exciter HQ500/20, emitter S535/30) (Chroma Technologies, USA). For the acceptor photobleaching experiment, YFP was bleached by continuous illumination of excitation at the maximal strength for 20 seconds.

Results

Morphology of dividing chloroplasts in *arc11*

Chloroplasts undergo active membrane expansion and division during development from undifferentiated proplastids in meristems (Pyke et al., 1999). In higher plants chloroplast division is not synchronized, which is evident from the variety of chloroplast division states visible in various tissues and cells (Fig. 1A). To efficiently characterize division states of *arc11* chloroplasts, we made use of hypocotyls and primary leaf petioles at an early stage of seedling development. Chlorophyll autofluorescence imaging by CLSM showed that a wide range of green tissues in *arc11* contain a decreased number of mostly elongated and expanded chloroplasts with irregular shapes as compared with wild-type (WT, *Ler*) tissues, which contain round to ellipsoidal or dumbbell-shaped chloroplasts (Fig. 1A). More detailed single chloroplast imaging using higher magnifications revealed that the morphological abnormalities of *arc11* chloroplasts are clearly linked to defects in division, as revealed by the existence of multiple constrictions (Fig. 1B; see also supplementary figure). Normal chloroplast division follows a coordinated pathway of events: slight envelope expansion, initial central constriction at a single site, further membrane constriction, and membrane fission as the final stage

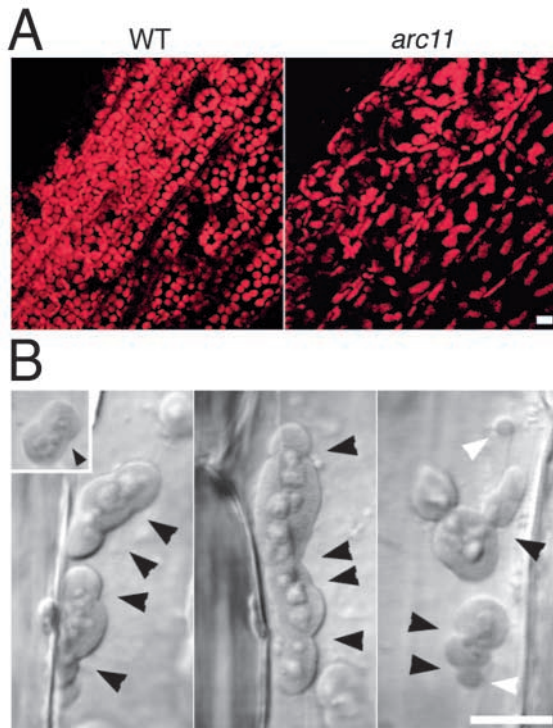


Fig. 1. The elongated and multiple-arrayed dividing chloroplasts in developing seedlings of *Arabidopsis arc11*. Chloroplasts in primary leaf petioles of 7-day light-grown wild-type (WT, *Ler*) and *arc11* seedlings were observed by CLSM. (A) Imaging of chlorophyll autofluorescence of WT and the *arc11*. (B) Differential interference contrast (DIC)-single optical sections of dividing chloroplasts in WT (inset) and *arc11*. Membrane constriction sites of dividing chloroplasts are indicated by black arrowheads. Mini-chloroplasts (~2 μm in diameter) in a population of expanding and dividing chloroplasts in *arc11* are indicated by white arrowheads. Bars, 10 μm .

(see Fig. 1B, inset). By contrast, *arc11* chloroplasts did not display a single central constriction but showed a varying number of constrictions from one to several, the most severe phenotype showing six constriction sites (Fig. 1B; see supplementary figure). Moreover, these constriction sites were placed randomly, but in parallel, along the long axis of chloroplasts (Fig. 1B). The arrayed chloroplast morphology indicates that membrane constriction in *arc11* initiates and proceeds regardless of division initiation at other sites. The asymmetrical placement of constriction sites and the continuing membrane expansion results in a heterogeneous population of chloroplasts in terms of size and shape, including spherical mini-chloroplasts less than 2 μm in diameter (Fig. 1B, white arrowhead). Despite this, the envelope membrane still appears to grow with polarity during the division process. In more mature cells such as mesophyll cells, multiple arrayed chloroplasts could not be detected, whereas elongated and filamentous chloroplasts could be observed (data not shown) as described previously (Marrison et al., 1999).

It is clear that *arc11* chloroplasts mislocalize the chloroplast division apparatus during division, a phenotype previously not reported. Furthermore, the observed phenotypes of dividing *arc11* chloroplasts show significant resemblance to the *min* mutants (Bi and Lutkenhaus, 1993), in addition to the observed

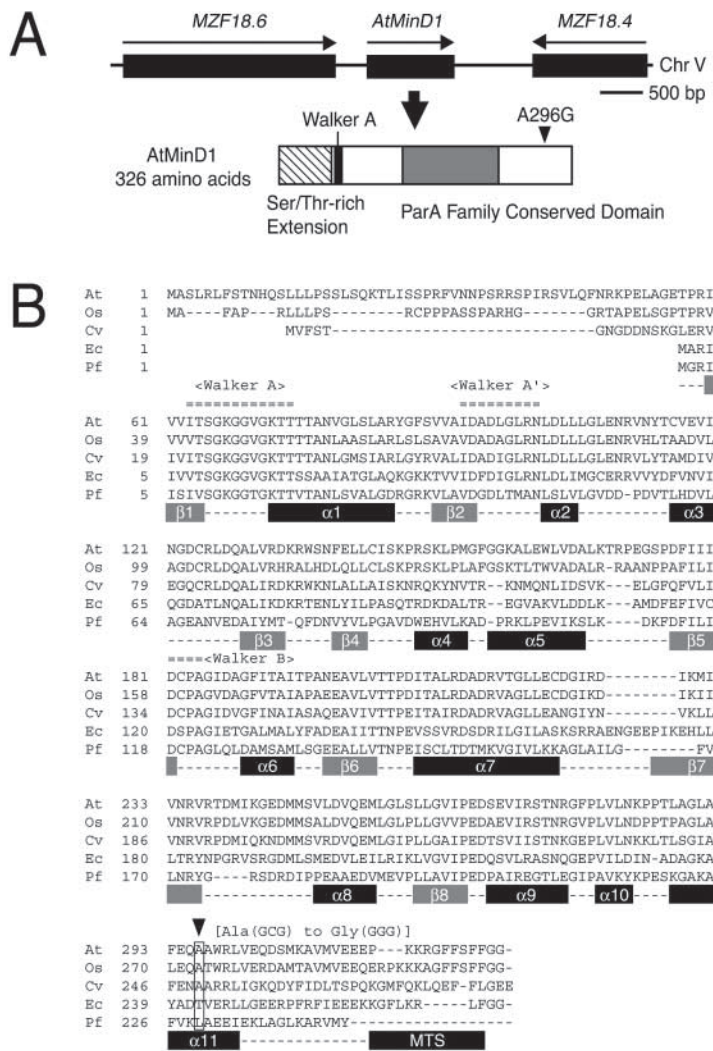
phenotype of *AtMinE1* overexpressing plants (Maple et al., 2002).

Sequence analysis and expression of *AtMinD1* in *arc11*

It was previously reported that the asymmetric division of *arc11* mesophyll chloroplasts showed similarity to the chloroplast morphology observed in *Arabidopsis AtMinD1* antisense plants (Colletti et al., 2000). Furthermore, the *arc11* locus was mapped close to the SSLP marker *nga139* on *Arabidopsis* chromosome V (Marrison et al., 1999), which is in close proximity to the *AtMinD1* locus (Fig. 2A). To examine our hypothesis that *arc11* could be allelic to *AtMinD1*, we investigated the expression profile and the DNA sequence of *AtMinD1* in *arc11*. Quantification of *AtMinD1* transcripts using *AtMinD1*/18S rRNA ratio calculations indicated that the transcript abundance in *Ler* and *arc11* seedlings is almost identical, with relative amounts of 1.40 ± 0.14 (*Ler*=1) (Fig. 3). However, *AtMinD1* sequence analysis in *Col*, *Ler* and *arc11* revealed that a single nucleotide substitution is present in *AtMinD1* in *arc11* (Fig. 2B). This cytosine to guanine nucleotide substitution results in a missense A296G mutation within α -helix 11 at the C-terminus of *AtMinD1* (Fig. 2). Interestingly, alignment analysis of MinD amino acid sequences from bacteria to plants revealed that Ala 296 shares limited conservation to green plants. Moreover, the recent crystal structure and functional analyses of bacterial MinD proteins (Cordell and Löwe, 2001; Hayashi et al., 2001; Sakai et al., 2001) has revealed that Ala 296 is located distantly from crucial motifs and amino acid residues important for direct nucleotide binding and interaction with MinC. To date, no functional implications have been reported for α -helix 11 in any species.

Genetic complementation of *arc11*

To test whether the *arc11* phenotype is indeed due to the A296G mutation in *AtMinD1*, we introduced a wild-type *AtMinD1* transgene into the nuclear genome of *arc11* plants. *AtMinD1* was expressed as a fusion with a 21-residue double hemagglutinin (dHA) epitope tag at its C-terminus under the control of the *AtMinD1* upstream genomic promoter sequence. In all, 55 T₁ plants were obtained, and chloroplast morphology and *AtMinD1* expression levels of these plants were examined (Figs 3, 4). In many plants partial or full complementation phenotypes could be observed at the T₁ generation, which was associated with T-DNA insertions; however, several T₂ and T₃ progenies displayed different chloroplast phenotypes between individuals (Fig. 4F,G; data not shown). By observing hygromycin resistance (T-DNA marker) in segregated plants this observation was most probably due to changes in genomic T-DNA copy number resulting in disequilibrium of the highly sensitive relationship between *AtMinD1* expression levels and chloroplast division (Colletti et al., 2000; Dinkins et al., 2001). Further microscopic characterizations established three independent transgenic lines showing stable complementation phenotypes at T₃ and T₄ generations (Fig. 4C), whereas more than ten lines showed an apparent division inhibition phenotype (Fig. 4D). Using immunoblot analysis and the anti-HA antibody we confirmed that the transgene in these transgenic lines produced the expected sized protein (data not



shown). Quantitative RT-PCR analyses of total and endogenous *AtMinD1* transcript levels confirmed that transgenic plants showing successful complementation (lines 11HA38 and 11HA42; Fig. 4C) displayed similar (0.96 to 2.82 times to that of WT *AtMinD1*) *AtMinD1* transgene expression levels to WT (Fig. 3). By contrast, the chloroplast division inhibition phenotype (lines 11HA2 and 11HA7; Fig. 4D) was associated with highly elevated transgene expression levels, consistent with previous observations (Fig. 3) (Colletti et al., 2000; Dinkins et al., 2001). Together, these findings show that *arc11* is a loss-of-function mutant of *AtMinD1* and that the observed phenotype is due to a single A296G mutation.

Fig. 2. Structure and the mutation point of *AtMinD1* in the *arc11*. (A) Chromosomal location of *AtMinD1* and domain structure of its product. (B) Sequence alignment of MinD proteins from *Arabidopsis* (At; database accession number AB030278), *Oryza sativa* (Os; AP001129), *Chlorella vulgaris* (Cv; AB001684), *Escherichia coli* (Ec; J03153) and *Pyrococcus furiosus* (Pf; NC_003413), with secondary structure elements based on structural (Hayashi et al., 2001; Sakai et al., 2001) and membrane localization analyses (Szeto et al., 2002; Hu and Lutkenhaus, 2003), and the PSIPRED secondary structure prediction program (<http://bioinf.cs.ucl.ac.uk/psipred/>). A single base substitution of *AtMinD1* at position Ala 296 in $\alpha 11$ helix, changing Ala(GCG) to Gly(GGG), is indicated by arrowheads (A,B) and boxed in (B). (C) Assignment of the *AtMinD1* N-terminal region responsible for chloroplast targeting by localization analysis of nonfused and *AtMinD1* N-terminus-fused (*AtMinD1*(1-64)) GFP. CLSM images of GFP (green), chlorophyll autofluorescence (Chl, red) and DIC are shown. Bar, 5 μ m.

Interestingly, the observed chloroplast phenotype in partially complemented plants implied that slightly elevated expression levels of *AtMinD1* have an effect on chloroplast envelope morphology (Fig. 4G,H). Several segregating individuals from original T₁ plant (line 11HA38) showed slight division inhibition and normal-to-larger chloroplasts, 6–9 μ m in diameter, within cells (Fig. 4G). These chloroplasts displayed low heterogeneity in terms of size; however, the chloroplasts showed abnormalities in terms of envelope morphology, exhibiting distorted or surface-rugged outlines (Fig. 4G). Quantitative RT-PCR analysis for stable transgenic plants (line 11HA44; Fig. 4H) revealed that this phenotype is attributed to moderately enhanced *AtMinD1* transgene expression (Fig. 3). This indicates that normal expression of *AtMinD1* may be important not only for appropriate chloroplast division but also for correct envelope morphology.

Inhibition of chloroplast division by overexpression of *AtMinD1*(A296G)

MinD is an inhibitory division protein and its overexpression prevents division in *Escherichia coli* and chloroplasts (de Boer et al., 1989; Colletti et al., 2000; Kanamaru et al., 2000; Dinkins et al., 2001). If the A296G mutation perturbs *AtMinD1* function, we would expect that *AtMinD1*(A296G) overproduction would not affect chloroplast division. To test this, we expressed *AtMinD1*(A296G) under the control of the CaMV35S promoter in WT plant (Fig. 5). A total of 20 *CaMV35S-AtMinD1*(A296G) transgenic plants were obtained and analyzed by microscopy and RT-PCR as described previously. From this analysis we found that the transgenic plants displayed division inhibition, producing a few but enlarged chloroplasts inside cells (Fig. 5B). In some cases the large chloroplasts seemed to be vacuolated, as observed in *arc11* and *arc11* transgenic plants (see Fig. 4D). Quantification of *AtMinD1* transcript levels showed that endogenous *AtMinD1* levels were not affected in the *AtMinD1*(A296G) transgenic plants, proving that the observed division inhibition is associated with *AtMinD1*(A296G) transgene expression. These results show that the *AtMinD1*(A296G) mutant protein has

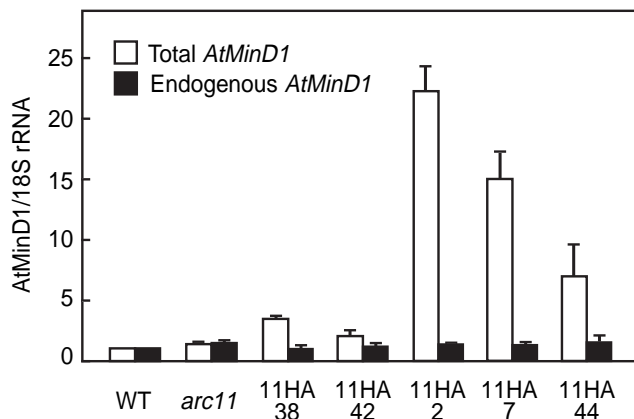


Fig. 3. Quantification of endogenous and total *AtMinD1* transcripts in *Arabidopsis* plants. Total RNAs from whole seedlings of *Arabidopsis* WT, *arc11* and transgenic *arc11* plants (11HA38 and 11HA42 as complemented lines, 11HA2 and 11HA7 as division-inhibited lines, 11HA44 as a partially complemented line, T₄ generation) harboring the *AtMinD1-dHA::Tnos* transgene were analyzed by TaqMan real-time quantitative RT-PCR system. Primer sets specific to the coding region and 3'-UTR of *AtMinD1* were employed to monitor total (white bars) and endogenous (black bars) *AtMinD1* transcript levels, respectively. Relative amounts of *AtMinD1* transcripts to 18S ribosomal RNA are shown as the means \pm s.e.m. (with WT=1) from three different plant samples.

retained its division inhibition activity but has lost its ability to control appropriate placement of the division apparatus.

Intraplasmidic localization patterns of *AtMinD1*(A296G) in vivo

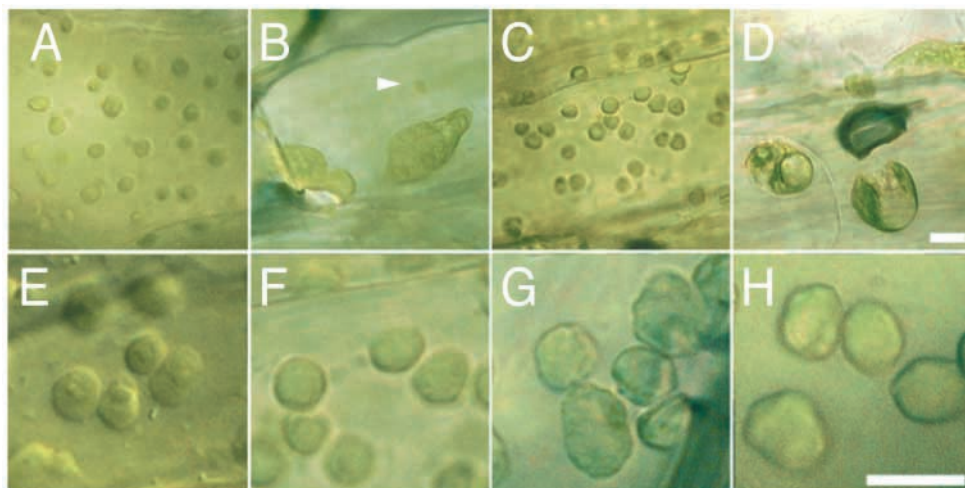
We previously reported that an *AtMinD1*-GFP fusion protein localizes to discrete speckle(s), which tend to localize as single spots at polar regions in ellipsoidal chloroplasts (Maple et al., 2002). To investigate the effect of the A296G mutation on intraplasmidic behavior of *AtMinD1*, we expressed an *AtMinD1*(A296G)-YFP fusion protein in live plant cells

(Fig. 6). As observed previously in transgenic plants, expression of a WT *AtMinD1*-GFP or *AtMinD1*-YFP fusion protein in leaf epidermal cells revealed discrete fluorescence signals to single stromal spots/speckles (Fig. 6; Table 1). By contrast, expression of an *AtMinD1*(A296G)-GFP or *AtMinD1*(A296G)-YFP fusion protein in leaf epidermal cells resulted in chloroplasts showing either large and distorted fluorescent aggregates and/or multiple speckles (Fig. 6; Table 1). These data show that the A296G mutation in *ARC11/AtMinD1* results in abnormal *AtMinD1* intraplasmidic localization patterns and implies an important role for α -helix 11 in terms of correct *AtMinD1* localization as part of the chloroplast division pathway.

Protein-protein interaction studies of *AtMinD1* using the yeast two-hybrid system

It has been shown that bacterial MinD forms dimers or polymers in the presence of ATP on the membrane (Hu et al., 2002; Suefujii et al., 2003), and it is possible that the intraplasmidic mislocalization of *AtMinD1*(A296G) inside chloroplasts is either due to loss of direct interaction with the envelope region itself or due to loss of protein-protein interaction capabilities. To gain further insights into this we examined protein-protein interactions of *AtMinD1* using the yeast two-hybrid system (Fig. 7). Full-length WT *AtMinD1* proteins were fused to the C-terminus of the Gal4 activation domain (AD-*AtMinD1*) and to the Gal4 DNA binding domain (BD-*AtMinD1*), respectively, and expressed in yeast AH109 cells. As a marker for protein-protein interactions we made use of the ability of AH109 to only grow in the absence of His on positive protein-protein interactions. We found that His auxotrophy was only restored in yeast cells cotransformed with both AD-*AtMinD1* and BD-*AtMinD1*, showing that *AtMinD1* can form homodimers (Fig. 7). The *AtMinD1* interaction appears to be relatively weak and/or transient in yeast cells, which was further verified by the observation that individual yeast transformants exhibited slightly different growth rates on His selection plates (data not shown). Although the *AtMinD1* interactions observed are relatively weak, repeated experiments

Fig. 4. Complementation of the *arc11* mutant with appropriate expression of wild-type *AtMinD1-dHA*. Chloroplasts in leaf petioles of 15-day seedlings were microscopically observed. (A) WT. (B) *arc11* mutant. A mini-chloroplast is indicated by an arrowhead. (C) Complemented *arc11* transgenic plant (11HA38, T₄ generation, see Fig. 3). (D) Division-inhibited *arc11* transgenic plant (11HA2, T₄ generation, see Fig. 3). (E-H) Partially complemented transgenic *arc11* plants containing slightly expanded and surface-rugged chloroplasts compared to WT and complemented plants. (E) WT. (F) Complemented plant (11HA38, identical to (C)). (G) A segregated plant of 11HA38 in the T₂ generation showing a partially complemented phenotype. (H) Partially complemented plant (11HA44, T₄ generation, see Fig. 3). Bars, 10 μ m.



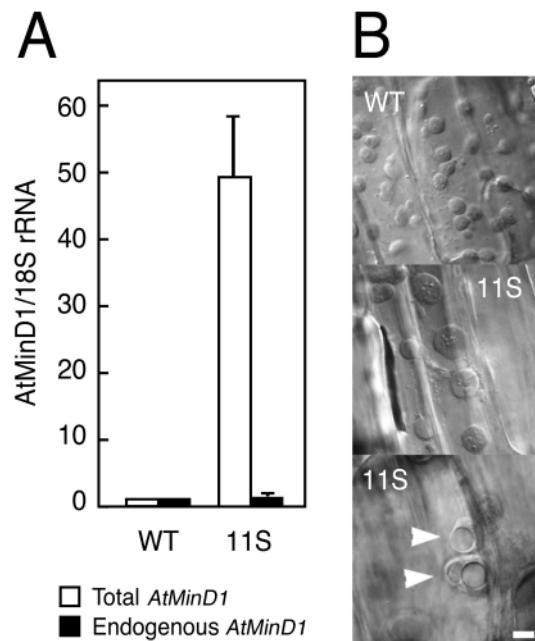


Fig. 5. Inhibition of chloroplast division by overexpression of *AtMinD1(A296G)* in transgenic *Arabidopsis*. (A) Relative amounts of total (white bars) and endogenous (black bars) *AtMinD1* transcripts to 18S ribosomal RNA analyzed by quantitative RT-PCR (see Fig. 3). Data are shown as the means \pm s.e.m. (with WT=1) from three different plant samples. (B) Images of chloroplasts in leaf petioles of WT and *CaMV35S-AtMinD1(A296G)* (11S) plants. Some populations of chloroplasts look vacuolated internally (arrowheads, see Fig. 4D). Bar, 10 μ m.

have conclusively confirmed that *AtMinD1* is capable of forming homodimers *in vivo*. In sharp contrast, His auxotrophy was not restored in yeast cells cotransformed with both AD-*AtMinD1* and BD-*AtMinD1(A296G)*, suggesting that the A296G mutation in *ARC11* abolishes its ability to form homodimers (Fig. 7). This was further confirmed by the lack of His auxotrophy restoration in yeast cells cotransformed with both AD-*AtMinD1(A296G)* and BD-*AtMinD1(A296G)*. Taken together, our results suggest that *AtMinD1* is capable of forming homodimers *in vivo* and that the loss of homodimerization of *AtMinD1* in *arc11* results in intraplasmidic mislocalization of *AtMinD1*, ultimately culminating in misplacement of the chloroplast division apparatus.

Protein-protein interaction of *AtMinD1* inside chloroplasts

To corroborate our yeast two-hybrid results we analyzed

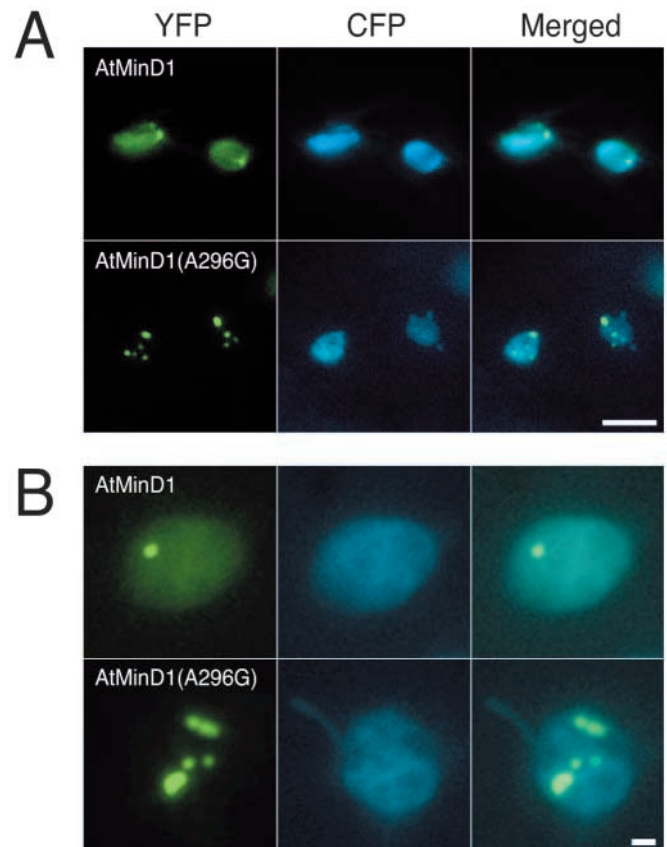


Fig. 6. Aberrant distribution of an *AtMinD1(A296G)*-YFP fusion protein inside chloroplasts. Expression vectors were introduced into young tobacco leaves by particle bombardment, and intraplasmidic fluorescent patterns of full-length *AtMinD1* and *AtMinD1(A296G)* proteins were analyzed. To visualize outlines of leaf epidermal chloroplasts, an expression vector for transit peptide-fused CFP was cotransformed. (A) Leaf epidermal chloroplasts containing YFP and CFP fluorescence. (B) Single chloroplast images at a higher magnification. Bars, 5 μ m (A) and 1 μ m (B).

AtMinD1 protein-protein interactions using Fluorescence Resonance Energy Transfer (FRET) technology (Gadella et al., 1999; Miyawaki and Tsien, 2000). FRET is an energy transfer process from a donor fluorophore to an acceptor fluorophore when donor and acceptor fluorophore are in close proximity (~ 100 Å); it has recently been utilized to analyze live cell events such as calcium ion dynamics and protein-protein interactions in planta (Gadella et al., 1997; Allen et al., 1999; Mas et al., 2000). On the basis of their spectroscopic properties cyan fluorescent protein (CFP) and yellow fluorescent protein (YFP) represent an ideal FRET fluorophore pair *in vivo*: energy flow from the donor

Table 1. Localization patterns of *AtMinD1*-GFP fusion proteins in tobacco leaf cells*

Protein	Number of cells	Number of speckles per chloroplast (%) [‡]						Total number of chloroplasts (%)
		0	1	2	3	4	>5	
<i>AtMinD1</i>	40	58 (15.8)	223 (60.9)	47 (12.8)	13 (3.6)	9 (2.5)	16 (4.4)	336 (100)
<i>AtMinD1(A296G)</i>	56	0 (0.0)	140 (31.9)	91 (20.7)	65 (14.8)	42 (9.6)	101 (23.0)	439 (100)

*The experiment was performed by particle bombardment using sections from single leaf.

[‡]Fluorescence speckles were counted by Nikon TE2000 microscope and Hamamatsu ORCA-ER cooled CCD camera and OpenLab software system.

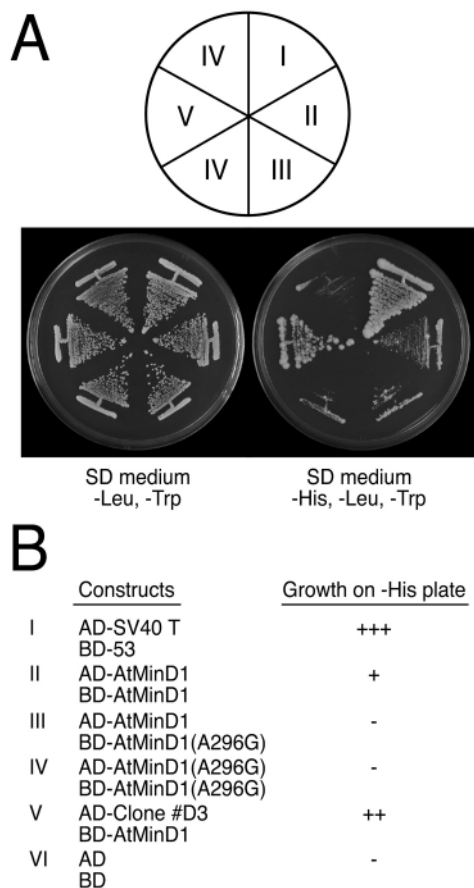


Fig. 7. Effect of the A296G mutation on AtMinD1 protein-protein interaction in the yeast two-hybrid system. AH109 cells harboring two expression vectors were grown on selection media plates at 30°C. (A) A 3-day plate lacking Leu and Trp (left) and a 5-day plate lacking His, Leu and Trp (right). (B) Growth of yeast cells on -His plates. Controls and classification of yeast growth are described in Materials and Methods.

(CFP) to the acceptor (YFP) enables capture of YFP emission upon CFP excitation. We constructed two vectors expressing AtMinD1 as a fusion to CFP and YFP and transiently expressed these in tobacco leaf cells by particle bombardment. As expected, both fusion proteins, in their respective CFP and YFP fluorescent channels, showed a discrete bright speckle(s) within chloroplasts (Fig. 8A), as observed with AtMinD1-YFP (Fig. 6). In cells where AtMinD1-CFP and AtMinD1-YFP were co-expressed, a significant increase in fluorescence intensity was observed upon CFP excitation in the FRET channel (excitation filter 436/10; emission filter 535/30) as compared with the signal (bleedthrough) when using single fluorescent protein fusions (Fig. 8A), suggesting that FRET occurs from the donor (AtMinD1-CFP) to the acceptor (AtMinD1-YFP) in chloroplasts. To verify these findings we performed acceptor photobleaching experiments (Miyawaki and Tsien, 1999) by applying high-intensity YFP excitation for a short time period to minimize chloroplast damage (Fig. 8B). After photobleaching a clear increase of the donor fluorescence (CFP) was observed in the fluorescent regions within chloroplasts (Fig. 8B), showing a reduction in energy transfer, which is diagnostic of FRET. We detected no increase in AtMinD1-CFP fluorescence by this

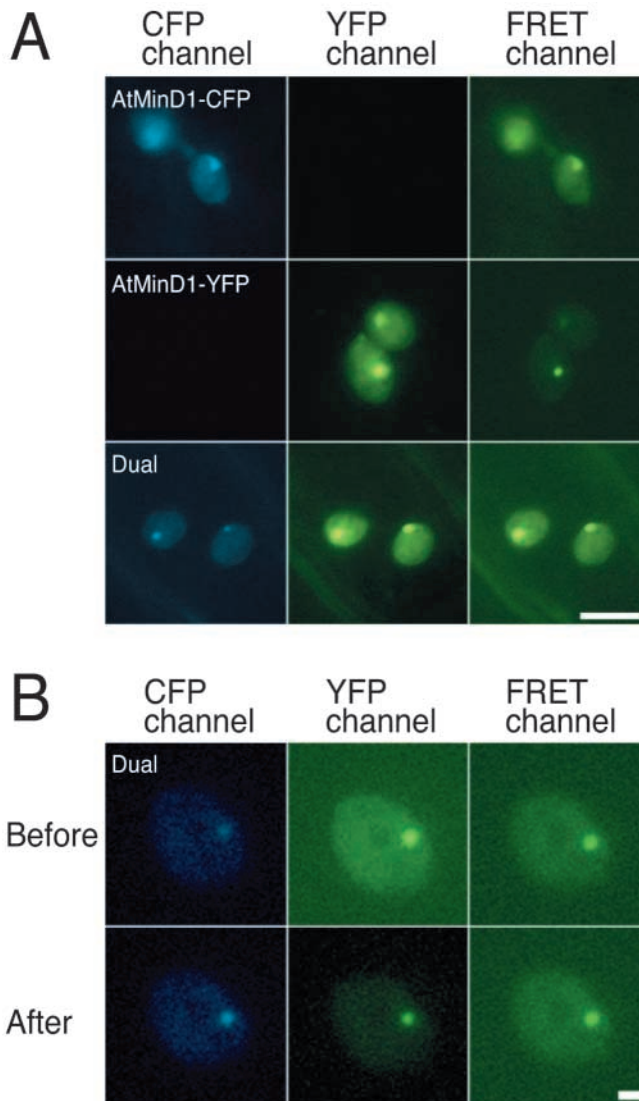


Fig. 8. FRET assay for AtMinD1 protein-protein interaction in chloroplasts. AtMinD1-CFP and/or AtMinD1-YFP were expressed in tobacco leaves by particle bombardment. Fluorescence of CFP and YFP in leaf epidermal chloroplasts was detected by epifluorescence microscopy. In the FRET channel, emission of YFP was detected upon CFP excitation. (A) Single and dual expression of fluorescent protein-tagged AtMinD1 proteins. (B) Moderate photobleaching of the acceptor YFP leading to the increased emission of CFP. All fluorescent images were taken at the same exposure time (200 milliseconds) using a 60× objective lens (Nikon). Emission signals of CFP (light blue) and YFP (yellowish green) are pseudo-colored. Bars, 5 μm (A) and 1 μm (B).

treatment in single fluorophore control experiments, but rather a fluorescence signal decrease as expected (data not shown). Thus, our data show that FRET occurred between AtMinD1-CFP and AtMinD1-YFP and that AtMinD1 proteins physically interact inside chloroplasts.

Discussion

arc11 contains multiple-arrayed chloroplasts

Although previous studies described asymmetrical, single

constriction sites during chloroplast division events in mesophyll cells of *arc11* and *AtMinD1* antisense plants (Marrison et al., 1999; Colletti et al., 2000), we have shown here that hypocotyls and petioles of young *arc11* seedlings contain mainly elongated and asymmetrically dividing multiple-arrayed chloroplasts (Fig. 1B; see supplementary figure). The observed differences between previous studies and our studies most probably reflect the use of different tissues at different stages of development. Multiple-arrayed chloroplasts have also been observed in hypocotyls of plants with elevated *AtMinE1* levels (Maple et al., 2002), and combined, these results suggest that elongating young tissues represent an excellent source for the observation of dividing chloroplasts in live cells.

The asymmetrical division and mini-chloroplast phenotype of *arc11* chloroplasts resembles that of the bacterial *min* phenotype, rather than the division-inhibited *filamentous* phenotype (de Boer et al., 1989). Our results expand and reinforce previous studies (Marrison et al., 1999; Colletti et al., 2000) which suggested that AtMinD1 represents a conserved chloroplast division component involved in the correct placement of the division machinery. The elongated morphology of *arc11* chloroplasts might be explained by polar membrane growth during chloroplast division and subsequent multiple division site formations. It has been indicated through physiological studies on the *arc* mutants that the relationship between division and envelope membrane expansion is independent and compensatory when one process is inhibited (Pyke, 1997). Division arrest or delays might therefore cause extended polar growth of envelope membranes; however, the biogenesis of multiple-arrayed chloroplasts is an issue that deserves further study.

AtMinD1 expression level-chloroplast phenotype relationship

arc11 was successfully complemented by the expression of *AtMinD1-dHA* at approximately equal levels to endogenous *AtMinD1* transcript levels observed in WT plants. Unexpectedly, we were only able to identify three transgenic plants showing a stable complementation phenotype. As most chloroplast division genes are known to affect chloroplast division as a result of their elevated or decreased expression levels, it is highly probable that regulatory elements, the chromosomal location and/or copy number of the *AtMinD1-dHA* T-DNA affect spatial and temporal expression patterns resulting in aberrant chloroplast division. Interestingly, observations of transgenic lines showing partial complementation and weak division inhibition suggested that regulated expression of *AtMinD1* may also be important in maintaining envelope membrane morphology (Fig. 4G,H). In partially complemented *arc11* plants the chloroplasts were relatively uniform in size, but on closer examination the chloroplast envelopes appeared both distorted and rugged on the surface (Fig. 4G,H) as compared with WT (Fig. 4E) and fully complemented lines (Fig. 4F). Although most known plants defective in chloroplast division display an abnormal chloroplast shape, the rugged chloroplast envelopes, as shown in Fig. 4G and 4H, were specific to the partially complemented *arc11* plants: examination of chloroplasts from *AtFtsZ* and *AtMinE1* transgenic plants and all the other 11 *arc* mutants did

not reveal rugged and distorted chloroplast envelopes (unpublished). It appears therefore that *AtMinD1* may affect the mechanism of controlling chloroplast envelope membrane morphology, either directly or indirectly, and that it is expression-level dependent.

The A296G point mutation in *AtMinD1* results in mislocalization and loss of dimerization capacity

The mutated amino acid residue in *arc11*, Ala 296, is a plant-specific conserved residue present in α -helix 11 (secondary elements are based on structural analyses of *Pyrococcus* MinD), which is absent in prokaryotic MinD proteins (Fig. 2B). α -helix 11 is close to the extreme C-terminal amphipathic helix, which is essential for membrane association of MinD in *E. coli* (Szeto et al., 2002; Hu and Lutkenhaus, 2003) (Fig. 2). Although no functional significance of α -helix 11 has to date been reported in either prokaryotic or eukaryotic MinD proteins, our results show that the A296G mutation in *AtMinD1* causes aberrant localization inside chloroplasts. In contrast to WT *AtMinD1*, which shows distinct single polar localization patterns, *AtMinD1*(A296G) localizes to multiple spots/speckles throughout the stroma and to large abnormal spots when expressed in WT leaf cells (Fig. 6; Table 1). This indicates that a disruption of α -helix 11 renders *AtMinD1* unable to localize appropriately. The A296G substitution in *AtMinD1* may either lead to an overall conformational change of the entire protein or to a more localized conformational change only affecting the C-terminal part of *AtMinD1*. We favor the latter, as *AtMinD1*(A296G) has retained chloroplast division inhibitory activity (Fig. 5) and because the extreme C-terminal part of MinD, which is conserved from eubacteria to chloroplasts, is surface exposed and responsible for membrane localization through an amphipathic helix in bacteria (Szeto et al., 2002; Hu and Lutkenhaus, 2003). It is possible that the introduction of a Gly residue in α -helix 11 results in helix disruption due to the great rotational freedom of Gly residues which, in turn, leads to a direct loss of appropriate localization inside chloroplasts.

Recent studies have shown that dimerization or polymerization of MinD is strictly ATP-dependent and is vital for MinD mode of action (Hu et al., 2002; Suefuji et al., 2003; Hu and Lutkenhaus, 2003). We have shown here that *AtMinD1* forms homodimers (Figs 7, 8) and that the A296G mutation results in the loss of *AtMinD1* dimerization capacity (Fig. 7), which ultimately results in division site misplacement (Fig. 1). Although unlikely, due to the distant localization of A296 to the nucleotide binding site in *AtMinD1*, it is possible that ATP binding is affected by the A296G mutation in *AtMinD1* resulting in loss of dimerization. Alternatively, and more probable, is that loss of dimerization capacity is due to a local C-terminal conformational disruption caused by the A296G substitution in *arc11*. This further suggests that the C-terminal region, and more specifically α -helix 11 of *AtMinD1*, is responsible for *AtMinD1* dimerization. This is in slight contrast to *E. coli* MinD, which requires its nucleotide binding domain for dimerization purposes. However, *E. coli* MinD dimerization most probably also requires amino acid residues distant to the nucleotide binding domain. Despite this, it is possible that MinD in plants has acquired new dimerization properties

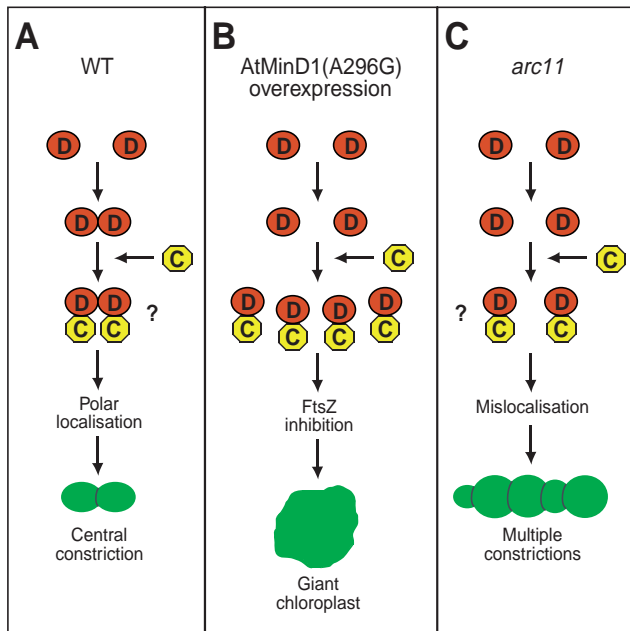


Fig. 9. A possible working model for AtMinD1-mediated chloroplast division site placement in chloroplasts. (A) In WT AtMinD1 displays functional dimerization and binds to a putative MinC-like protein (?) followed by appropriate polar localization. This ensures correct division machinery placement resulting in a single central constriction site. (B) In AtMinD1(A296G) overexpressing plants, the mutated protein is unable to form dimers but can 'activate' a putative MinC-like protein (?) resulting in FtsZ polymerization inhibition and division arrest. (C) In *arc11* chloroplasts AtMinD1(A296G) does not dimerize but binds a putative MinC-like protein (?) and due to its mislocalization inappropriate division machinery placement takes place, resulting in multiple constriction site formation.

from other ATPases different from that of classical prokaryotic MinD proteins during evolution generating an evolutionary MinD hybrid. For example, the NifH ATPase shows a good fit when superimposed on the *E. coli* MinD structure and NifH contains a C-terminal surface-exposed α -helical region, absent in *E. coli* MinD, involved in NifH dimerization (Lutkenhaus and Sundaramoorthy, 2003). It is possible that AtMinD1 represents an evolutionary protein hybrid containing both classical prokaryotic MinD domains in addition to domains acquired from other P-loop ATPases.

In prokaryotic systems it is not known whether MinD dimerization occurs after or before membrane association, and although we favor the hypothesis that AtMinD1 forms dimers before localization, it is possible that appropriate AtMinD1 localization occurs before dimerization. This is an area that requires further study.

A working model for AtMinD1-mediated division machinery placement in chloroplasts

We have shown that AtMinD1 displays functional dimerization (Figs 7, 8) and we suggest that AtMinD1 dimerization is important for correct intraplasmidic localization patterns (Fig. 6). In *E. coli* it is proposed that MinD-mediated division site placement follows a coordinated sequence of events: MinD

forms homodimers when bound to ATP; MinD then interacts with the FtsZ polymerization inhibitor MinC and moves to the membrane; MinE then interacts with the MinCD complex and stimulates ATP hydrolysis and membrane release (Lutkenhaus and Sundaramoorthy, 2003). Although no MinC protein has been identified in plants we propose that a MinC-like division inhibitor is probably present in *Arabidopsis* because overexpression of WT AtMinD1 in *Arabidopsis* results in chloroplast division inhibition (Colletti et al., 2000; Kanamaru et al., 2000; Dinkins et al., 2001) (Figs 3, 4), which is suggestive of excessive MinC-like protein activation and loss of FtsZ polymerization. On the basis of these data and our findings presented here, we propose a new working model for AtMinD1-mediated chloroplast division site placement in *Arabidopsis* (Fig. 9). In WT plants AtMinD1 forms dimers inside chloroplasts followed by recruitment and activation of a putative MinC-like protein. Following this the protein complex mediates appropriate placement of the division machinery, ensuring a single central constriction site by inhibiting FtsZ polymerization at inappropriate sites (Fig. 9A). In *arc11* chloroplasts AtMinD1 is unable to form dimers (Fig. 9C) but retains its ability to interact with a putative division inhibitor protein as indicated by the loss of division site formation in *arc11* overexpressing plants (Fig. 9B). This leads to mislocalization of the protein complex, ultimately resulting in division site misplacement and multiple constriction sites (Fig. 9C).

We have shown here that AtMinD1-mediated division site placement in *Arabidopsis* chloroplasts follows a coordinated sequence of events. Although a MinC-like protein remains to be identified in plants, this initial insight into the molecular machinery controlling division site placement in *Arabidopsis* chloroplasts has paved the way for new findings into the fundamental biological process of chloroplast division.

The authors thank Arabidopsis Biological Resource Center (Ohio State University, USA) and Joanne L. Marrison and Rachel M. Leech (University of York, UK) for providing the *arc11* seeds, Masanobu Nakamura (University of Tokyo, Japan) and Akira Nagatani (Kyoto University, Japan) for the pBI-Hyg/35S-NosT vector, and Yasuo Niwa (University of Shizuoka, Japan) for the CaMV35S-sGFP(S65T)-nos vector. We also thank members of the Yoshida and the Møller laboratories for helpful discussions and technical assistance. This work was in part supported by Grants-in-Aid 14760068 from the Ministry of Education, Culture, Sports, Science and Technology of Japan to M.T.F., grants from the Special Postdoctoral Research Program of RIKEN to M.T.F. and R.I., and from BBSRC (91/C17189 and 91/RE118421), The Royal Society (574006.G503/23280/SM) and HEFCE (HIRF/046) to S.G.M.

References

- Allen, G. J., Kwak, J. M., Chu, S. P., Llopis, J., Tsien, R. Y., Harper, J. F. and Schroeder, J. I. (1999). Cameleon calcium indicator reports cytoplasmic calcium dynamics in *Arabidopsis* guard cells. *Plant J.* **19**, 735-747.
- Beech, P. L., Nheu, T., Schultz, T., Herbert, S., Lithgow, T., Gilson, P. R. and McFadden, G. I. (2000). Mitochondrial FtsZ in a chromophyte alga. *Science* **287**, 1276-1279.
- Bi, E. and Lutkenhaus, J. (1991). FtsZ ring structure associated with division in *Escherichia coli*. *Nature* **354**, 161-164.
- Bi, E. and Lutkenhaus, J. (1993). Cell division inhibitors SulA and MinCD prevent formation of the FtsZ ring. *J. Bacteriol.* **175**, 1118-1125.
- Clough, S. J. and Bent, A. F. (1998). Floral dip: a simplified method for

- Agrobacterium*-mediated transformation of *Arabidopsis thaliana*. *Plant J.* **16**, 735-743.
- Colletti, K. S., Tattersall, E. A., Pyke, K. A., Froelich, J. E., Stokes, K. D. and Osteryoung, K. W.** (2000). A homologue of the bacterial cell division site-determining factor MinD mediates placement of the chloroplast division apparatus. *Curr. Biol.* **10**, 507-516.
- Cordell, S. C. and Löwe, J.** (2001). Crystal structure of the bacterial cell division regulator MinD. *FEBS Lett.* **492**, 160-165.
- de Boer, P. A. J., Crossley, R. E. and Rothfield, L. I.** (1989). A division inhibitor and a topological specificity factor coded for by the minicell locus determine proper placement of the division septum in *E. coli*. *Cell* **56**, 641-649.
- de Boer, P. A., Crossley, R. E., Hand, A. R. and Rothfield, L. I.** (1991). The MinD protein is a membrane ATPase required for the correct placement of the *Escherichia coli* division site. *EMBO J.* **10**, 4371-4380.
- Dinkins, R., Reddy, M. S., Leng, M. and Collins, G. B.** (2001). Overexpression of the *Arabidopsis thaliana* *MinD1* gene alters chloroplast size and number in transgenic tobacco plants. *Planta* **214**, 180-188.
- Erickson, H. P., Taylor, D. W., Taylor, K. A. and Bramhill, D.** (1996). Bacterial cell division protein FtsZ assembles into protofilament sheets and mini-rings, structural homologs of tubulin polymers. *Proc. Natl. Acad. Sci. USA* **93**, 519-523.
- Fu, X., Shih, Y.-L., Zhang, Y. and Rothfield, L. I.** (2001). The MinE ring required for proper placement of the division site is a mobile structure that changes its cellular location during the *Escherichia coli* division cycle. *Proc. Natl. Acad. Sci. USA* **98**, 980-985.
- Fujiwara, M. and Yoshida, S.** (2001). Chloroplast targeting of chloroplast division FtsZ2 proteins in *Arabidopsis*. *Biochem. Biophys. Res. Commun.* **287**, 462-467.
- Fulgosi, H., Gerdes, L., Westphal, S., Glockmann, C. and Soll, J.** (2002). Cell and chloroplast division requires ARTEMIS. *Proc. Natl. Acad. Sci. USA* **99**, 11501-11506.
- Gadella, T. W., Jr, Vereb, G., Jr, Hadri, A. E., Rohrig, H., Schmidt, J., John, M., Schell, J. and Bisseling, T.** (1997). Microspectroscopic imaging of nodulation factor-binding sites on living *Vicia sativa* roots using a novel bioactive fluorescent nodulation factor. *Biophys. J.* **72**, 1986-1996.
- Gadella, T. W. J., Jr, Van der Krogt, G. N. M. and Bisseling, T.** (1999). GFP-based FRET microscopy in living plant cells. *Trends Plant Sci.* **4**, 287-291.
- Gao, H., Kadirjan-Kalbach, D., Froehlich, J. E. and Osteryoung, K. W.** (2003). ARC5, a cytosolic dynamin-like protein from plants, is part of the chloroplast division machinery. *Proc. Natl. Acad. Sci. USA* **100**, 4328-4333.
- Gray, M. W.** (1999). Evolution of organellar genomes. *Curr. Opin. Genet. Dev.* **9**, 678-687.
- Hale, C. A., Meinhardt, H. and de Boer, P. A. J.** (2001). Dynamic localization cycle of the cell division regulator MinE in *Escherichia coli*. *EMBO J.* **20**, 1563-1572.
- Hashimoto, H.** (2003). Plastid division: its origins and evolution. *Int. Rev. Cytol.* **222**, 63-98.
- Hayashi, I., Oyama, T. and Morikawa, K.** (2001). Structural and functional studies of MinD ATPase: implications for the molecular recognition of the bacterial cell division apparatus. *EMBO J.* **20**, 1819-1828.
- Hu, Z. and Lutkenhaus, J.** (2001). Topological regulation of cell division in *E. coli*. spatiotemporal oscillation of MinD requires stimulation of its ATPase by MinE and phospholipid. *Mol. Cell* **7**, 1337-1343.
- Hu, Z. and Lutkenhaus, J.** (2003). A conserved sequence at the C-terminus of MinD is required for binding to the membrane and targeting MinC to the septum. *Mol. Microbiol.* **47**, 345-355.
- Hu, Z., Mukherjee, A., Pichoff, S. and Lutkenhaus, J.** (1999). The MinC component of the division site selection system in *Escherichia coli* interacts with FtsZ to prevent polymerization. *Proc. Natl. Acad. Sci. USA* **96**, 14819-14824.
- Hu, Z., Gogol, E. P. and Lutkenhaus, J.** (2002). Dynamic assembly of MinD on phospholipid vesicles regulated by ATP and MinE. *Proc. Natl. Acad. Sci. USA* **99**, 6761-6766.
- Huang, J. and Lutkenhaus, J.** (1996). Interaction between FtsZ and inhibitors of cell division. *J. Bacteriol.* **178**, 5080-5085.
- Itoh, R., Fujiwara, M., Nagata, N. and Yoshida, S.** (2001). A chloroplast protein homologous to the eubacterial topological specificity factor MinE plays a role in chloroplast division. *Plant Physiol.* **127**, 1644-1655.
- Kanamaru, K., Fujiwara, M., Kim, M., Nagashima, A., Nakazato, E., Tanaka, K. and Takahashi, H.** (2000). Chloroplast targeting, distribution and transcriptional fluctuation of AtMinD1, a eubacteria-type factor critical for chloroplast division. *Plant Cell Physiol.* **41**, 1119-1128.
- Kost, B., Spielhofer, P. and Chua, N. H.** (1998). A GFP-mouse talin fusion protein labels plant actin filaments *in vivo* and visualises the actin cytoskeleton in growing pollen tubes. *Plant J.* **16**, 393-401.
- Kuroiwa, T., Kuroiwa, H., Sakai, A., Takahashi, H., Toda, K. and Itoh, R.** (1998). The division apparatus of plastids and mitochondria. *Int. Rev. Cytol.* **181**, 1-41.
- Kuroiwa, H., Mori, T., Takahara, M., Miyagishima, S. and Kuroiwa, T.** (2002). Chloroplast division machinery as revealed by immunofluorescence and electron microscopy. *Planta* **215**, 185-190.
- Leech, R. M. and Pyke, K. A.** (1988). Chloroplast division in higher plants with particular reference to wheat. In *Division and Segregation of Organelles* (ed. S. A. Boffey and D. Lloyd), pp. 39-62. Cambridge: Cambridge University Press.
- Lutkenhaus, J. and Sundaramoorthy, M.** (2003). MinD and role of the deviant Walker A motif, dimerization and membrane binding in oscillation. *Mol. Microbiol.* **48**, 295-303.
- Maple, J., Chua, N. H. and Møller, S. G.** (2002). The topological specificity factor AtMinE1 is essential for correct plastid division site placement in *Arabidopsis*. *Plant J.* **31**, 269-277.
- Margolin, W.** (2001). Spatial regulation of cytokinesis in bacteria. *Curr. Opin. Microbiol.* **4**, 647-652.
- Marrison, J. L., Rutherford, S. M., Robertson, E. J., Lister, C., Dean, C. and Leech, R. M.** (1999). The distinctive roles of five different ARC genes in the chloroplast division process in *Arabidopsis*. *Plant J.* **18**, 651-662.
- Martin, W., Rujan, T., Richly, E., Hansen, A., Cornelsen, S., Lins, T., Leister, D., Stoebe, B., Hasegawa, M. and Penny, D.** (2002). Evolutionary analysis of *Arabidopsis*, cyanobacterial, and chloroplast genomes reveals plastid phylogeny and thousands of cyanobacterial genes in the nucleus. *Proc. Natl. Acad. Sci. USA* **99**, 12246-12251.
- Mas, P., Devlin, P. F., Panda, S. and Kay, S. A.** (2000). Functional interaction of phytochrome B and cryptochrome 2. *Nature* **408**, 207-211.
- Miyagishima, S., Nishida, K., Mori, T., Matsuzaki, M., Higashiyama, T., Kuroiwa, H. and Kuroiwa, T.** (2003). A plant-specific dynamin-related protein forms a ring at the chloroplast division site. *Plant Cell* **15**, 655-665.
- Miyawaki, A. and Tsien, R. Y.** (2000). Monitoring protein conformations and interactions by fluorescence resonance energy transfer between mutants of green fluorescent protein. *Methods Enzymol.* **327**, 472-500.
- Niwa, Y., Hirano, T., Yoshimoto, K., Shimizu, M. and Kobayashi, H.** (1999). Non-invasive quantitative detection and applications of non-toxic, S65T-type green fluorescent protein in living plants. *Plant J.* **18**, 455-463.
- Osteryoung, K. W. and Vierling, E.** (1995). Conserved cell and organelle division. *Nature* **376**, 473-474.
- Osteryoung, K. W., Stokes, K. D., Rutherford, S. M., Percival, A. L. and Lee, W. Y.** (1998). Chloroplast division in higher plants requires members of two functionally divergent gene families with homology to bacterial *ftsZ*. *Plant Cell* **10**, 1991-2004.
- Pyke, K. A.** (1997). The genetic control of plastid division in higher plants. *Am. J. Bot.* **84**, 1017-1027.
- Pyke, K. A.** (1999). Plastid division and development. *Plant Cell* **11**, 549-556.
- Raskin, D. M. and de Boer, P. A. J.** (1997). The MinE ring: an FtsZ-independent cell structure required for selection of the correct division site in *E. coli*. *Cell* **91**, 685-694.
- Raskin, D. M. and de Boer, P. A. J.** (1999). Rapid pole-to-pole oscillation of a protein required for directing division to the middle of *Escherichia coli*. *Proc. Natl. Acad. Sci. USA* **96**, 4971-4976.
- Rothfield, L., Justice, S. and Garcia-Lara, J.** (1999). Bacterial cell division. *Annu. Rev. Genet.* **33**, 423-448.
- Sakai, N., Yao, M., Itoh, H., Watanabe, N., Yumoto, F., Tanokura, M. and Tanaka, I.** (2001). The three-dimensional structure of septum site-determining protein MinD from *Pyrococcus horikoshii* OT3 in complex with Mg-ADP. *Structure* **9**, 817-826.
- Shimada, Y., Goda, H., Nakamura, A., Takatsuto, S., Fujioka, S. and Yoshida, S.** (2003). Organ-specific expression of brassinosteroid-biosynthetic genes and distribution of endogenous brassinosteroids in *Arabidopsis*. *Plant Physiol.* **131**, 287-297.
- Strepp, R., Scholz, S., Kruse, S., Speth, V. and Reski, R.** (1998). Plant nuclear gene knockout reveals a role in plastid division for the homolog of the bacterial cell division protein FtsZ, an ancestral tubulin. *Proc. Natl. Acad. Sci. USA* **95**, 4368-4373.
- Suefuji, K., Valluzzi, R. and RayChaudhuri, D.** (2003). Dynamic assembly of MinD into filament bundles modulated by ATP, phospholipids, and MinE. *Proc. Natl. Acad. Sci. USA* **99**, 16776-16781.

- Szeto, T. H., Rowland, S. L., Rothfield, L. I. and King, G. F.** (2002). Membrane localization of MinD is mediated by a C-terminal motif that is conserved across eubacteria, archaea, and chloroplasts. *Proc. Natl. Acad. Sci. USA* **99**, 15693-15698.
- Vitha, S., McAndrew, R. S. and Osteryoung, K. W.** (2001). FtsZ ring formation at the chloroplast division site in plants. *J. Cell Biol.* **153**, 111-119.
- Vitha, S., Froehlich, J. E., Koksharova, O., Pyke, K. A., van Erp, H. and Osteryoung, K. W.** (2003). ARC6 is a J-domain plastid division protein and an evolutionary descendant of the cyanobacterial cell division protein Ftn2. *Plant Cell* **15**, 1918-1933.
- Yamaguchi, R., Nakamura, M., Mochizuki, N., Kay, S. A. and Nagatani, A.** (1999). Light-dependent translocation of a phytochrome B-GFP fusion protein to the nucleus in transgenic *Arabidopsis*. *J. Cell Biol.* **145**, 437-445.